Adapting Transmitter Power and Modulation Format to Improve Optical Network Performance Utilizing the Gaussian Noise Model of Nonlinear Impairments

David J. Ives, *Member, OSA*, Polina Bayvel, *Fellow, IEEE*, and Seb J. Savory, *Senior Member, IEEE*

Abstract—This paper serves to highlight the gains in SNR margin and/or data capacity that can be achieved through a proper optimization of the transceiver parameters, for example, launch power, modulation format, and channel allocation. A simple quality of transmission estimator is described that allows a rapid estimation of the signal quality based on ASE noise and nonlinear interference utilizing the Gaussian noise model. The quality of transmission estimator was used to optimize the SNR and maximise the data throughput of transmission signals in a point-to-point link by adjusting the launch power and modulation format. In a three-node network, the launch power and channel allocation were adjusted to minimise the overall effect of nonlinear interference. This paper goes on to show that by optimizing the transceiver modulation format as part of the channel allocation and routing problem gains in network data throughput can be achieved for the 14-node NSF mesh network.

Index Terms—Adaptive modulation, Gaussian noise model, network optimization, nonlinear capacity, optical fiber communications.

I. INTRODUCTION

OPTICAL networks form the backbone of the internet. The demand for data transmission services is exponentially increasing with internet traffic continuing to double every 16 months [1], [2]. With the ever increasing number and variety of devices, and the ease with which users can both upload and download bandwidth-demanding content, such as video, this trend is likely to continue [3]. This has motivated the research into how the capacity of the optical network can be maximized.

Conventional wavelength routed optical networks, WRONs [4], allow the mapping of demand to transparently-routed lightpaths but their analysis has been limited to minimizing wavelength resources without taking individual physical channel properties into account. In these networks, it has been assumed that transceivers would be designed for error-free transmission, for all possible routing and re-routing scenarios, with an associated power budget to satisfy SNR requirements for the longest point-to-point link. Thus, for the majority of other routes there will be excessive margins, and a subsequent under-utilization of the available network resources. Recently, to improve network utilization the concept of elastic optical networks [5], [6] has attracted attention as spectral resource could be more flexibly allocated to the variable demands. Elastic optical networks have been extended to include modulation format adaption [7], [8], with the aim of improving further the overall, network-wide spectral efficiency. This work has been stimulated by the development of software-defined transceivers [9]–[11] which allow for dynamic optimization of a transmission link through the variation of both power and modulation formats. The integration of the transceiver and physical link parameters within the routing and spectrum assignment algorithm can potentially allow more efficient use of the network resources leading to higher data throughput and/or improved quality of transmission and forms the focus of the work in this paper.

Whilst significant research has already been carried out on improving network resource utilization, taking physical transmission characteristics into account, much of it has focused on mixed line rate networks, utilizing both coherent and incoherent transmission formats. The majority of mixed line rate optimization has only considered linear impairments. Nonlinear impairments caused by XPM have been included in [12] but the mix of coherent and incoherent formats dominates the impairment. It has been shown that it is possible to achieve significant saving in capital expenditure by matching transmission equipment to network demand [13] or through power optimization for the different transmission formats [14]. The work described in this paper has focused on using polarization-multiplexed coherent transmission formats in dispersion-uncompensated networks, where linear impairments can be equalized in the receiver and a simpler nonlinear impairment estimation based on the Gaussian noise model can be used [15].

This paper intends to study the benefits of and strategies for individual launch power optimization and channel allocation in terms of quality of transmission extending our work in [16] by studying a simple point-to-point link and a three node network with signals occupying the full c-band. The advantageous quality of transmission for shorter connections is used to allow the adaption of the modulation format allowing higher data transmission rates. The gains in the network data throughput of a wavelength routed transparent optical mesh network are studied for modulation adaption based on the quality of transmission and focus on maximizing the total data throughput rather than minimizing the cost for a specific network demand.

The rest of this paper is arranged as follows. In Section II we describe the computationally simple model of signal transmission quality in the weakly nonlinear propagation regime. The model is used in the following sections to optimize the transmitter launch power and format. In Section III the advantages of optimization in terms of SNR margin and capacity of a simple DWDM transmission link are explored. Building on this in Section IV we look at the SNR margin and capacity advantages from optimization in a three node network where there are different transmission distances. Finally in Section V the model is used to estimate the SNR of routes through a 14 node mesh network and use this to optimize the transmission format. The gain in overall network throughput for an optimally routed static traffic distribution is shown as the transmission formats are changed from a network wide fixed format to a route SNR adapted format.

II. NONLINEAR TRANSMISSION MODEL

Consider a polarization multiplexed coherent transmission system where the symbol SNR is limited by ASE noise and nonlinear interference. For an uncompensated link the nonlinear interference between DWDM channels caused by the Kerr effect can be considered as a source of additive Gaussian noise [17]–[20] and combines incoherently with the additive white Gaussian noise due to ASE. This is the so called Gaussian noise model of nonlinear interference. While recently a number of authors [21]–[23] have proposed correction terms to the GN model, for continental scale long haul network level simulations the assumptions of the GN model are valid and as such, similar to other authors [24] we utilise the simpler GN model under the assumption that it conservatively estimates the nonlinear interference noise and thus allows for robust network optimization. The symbol SNR, SNR_i, of the ith DWDM channel is given by

$$\text{SNR}_i = \frac{p_i}{n_{\text{ASE,i}} + n_{\text{NLI,i}}} \tag{1}$$

where p_i is the received signal power, $n_{\text{ASE,i}}$ is the ASE noise power and $n_{\text{NLI,i}}$ is the nonlinear interference noise power within the receiver filter bandwidth, all on the ith DWDM channel. It is assumed that the transmission loss is fully compensated by erbium doped fiber amplifiers, EDFA, so that the receive signal power is equal to the transmitter launch power and the ASE noise power is given by [25], [26]

$$n_{\text{ASE,i}} = 10^{\frac{\text{NF}}{10}} h\nu R \sum_k 10^{\frac{A_k}{10}} \tag{2}$$

where the summation, k, is taken over all EDFAs in the signal optical path, NF is the amplifier noise figure (dB), h is Planck's constant (6.626×10^{-34} J·s), ν is the channel carrier optical frequency (Hz), R is the symbol rate (baud) and A_k are the individual transmission losses (dB) between the $(k-1)^{\text{th}}$ and k^{th} EDFA. The effective receiver noise bandwidth used is equal to the symbol rate R under the assumption that the overall noise spectrum is white, dominated by ASE, and the receiver implements an ideal matched filter to maximize the SNR. The transmission losses A_k include the fiber span losses and ROADM losses. This approximation for the ASE noise assumes that the

gain of the amplifier is large and that any reduction in gain needed to match the span loss is achieved using a following variable attenuator.

The nonlinear interference noise can be considered as self phase modulation, SPM, for nonlinear interference caused solely within the ith channel, cross phase modulation, XPM, for interference on the ith channel caused by signals in the jth channel and four wave mixing, FWM, for interference caused by signals in multiple channels. For well spaced channels, such that there is minimal cross talk of the nonlinear interference noise between channels, and under the assumption that the nonlinear interference noise due to FWM can be ignored as insignificant [18] then the the nonlinear interference noise, $n_{\text{NLI,i}}$ on the ith channel due to SPM and XPM can be written as [16], [27]

$$n_{\text{NLI,i}} = p_i \sum_j X_{i,j} p_j^2 \tag{3}$$

where p are the channel launch powers and the summation j is over all, 80, channels, $X_{i,j}$ is the accumulated efficiency factor of the nonlinear interference on the ith channel caused by the jth interfering channel. $X_{i,j}, i \neq j$ is a XPM factor and $X_{i,i}$ is a SPM factor. SPM is included in this work, in contrast to our previous work [16], to give a more robust estimation of the nonlinear interference for the long transmission lengths considered here.

The efficiency factor, $X_{i,j}$, depends on the frequency spacing between channels i and j, the spectral shape of the channel, its symbol rate and the linear and nonlinear transmission properties of the optical fiber. For similar channels on a fixed regularly spaced frequency grid $X_{i,j} = X_{|i-j|}$. It is independent of the exact modulation format subject to the general assumption of it being a polarization multiplexed coherent transmission format. In order to calculate the efficiency factor $X_{i,j}$ consider just two DWDM channels with the same spectral shapes, such that the signal spectrum can be written as $G(f) = p_0 g(f) + p_1 g(f - \Delta f)$ where p_0 is the total launch power in the data channel, p_1 is the total launch power in the interfering channel, $g(f)$ is the power spectral shape of the channel normalized such that $\int g(f)df = 1$ and Δf is the channel separation. $g(f)$ is centered around $f = 0$ and assumed to fall entirely within a single DWDM channel. The nonlinear interference power spectral density G_{NLI} is given by the Gaussian noise reference equation (1) from [15]

$$G_{\text{NLI}}(f) = \frac{16}{27} \gamma^2 L_{eff}^2 \int_{-\infty}^{\infty} \int_{-\infty}^{\infty} \rho(f_1, f_2, f) \chi(f_1, f_2, f)$$
$$\cdot G(f_1) G(f_2) G(f_1 + f_2 - f) \, df_1 \, df_2 \tag{4}$$

where γ is the fiber nonlinearity coefficient (W^{-1}·km^{-1}), L_{eff} is the fiber effective nonlinear length (km), ρ represents the normalised nonlinear mixing efficiency [15] and χ is the "phased-array factor" for the coherent addition of noise from multiple spans [15]. The triple multiple in the integral of equation (4) has eight cross terms but only three of these terms produce interference noise within the data channel bandwidth, a single SPM term and two degenerate XPM terms. Thus the nonlinear

interference spectral power density due to XPM is given by

$$G_{\text{XPM}}(f) = 2\frac{16}{27}\gamma^2 L_{\text{eff}}^2 p_0 p_1^2$$

$$\int_{-\infty}^{\infty}\int_{-\infty}^{\infty} \rho(f_1, f_2, f)\chi(f_1, f_2, f)$$

$$g(f_1 - \Delta f)g(f_2)g(f_1 - \Delta f + f_2 - f)\, df_1\, df_2 \tag{5}$$

and that due to SPM is half this with $p_1 = p_0$ and Δf set to zero.

This noise spectral power density will be filtered in the coherent receiver by a matching filter to maximize the SNR. Provided the overall noise is dominated by additive white Gaussian noise, caused by ASE, the matching filter is given by $H(f) = R\,g(f)$ where R is the symbol rate. Making the simplification that the nonlinear interference noise of multiple spans can be added incoherently [28] such that $\chi(f_1, f_2, f) = N_s$, the number of transmission spans and also putting $\dot{f}_1 = f_1 - \Delta f - f$ and $\dot{f}_2 = f_2 - f$ we can write the nonlinear interference noise due to XPM, n_{XPM} as

$$n_{\text{XPM}} = p_0\, p_1^2\, X_{0,1} = p_0\, p_1^2\, N_s \frac{32}{27}\gamma^2\, R$$

$$\int_{-\infty}^{\infty}\int_{-\infty}^{\infty}\int_{-\infty}^{\infty} \frac{1 + e^{-2L\alpha} - 2e^{-L\alpha}\cos[4\pi^2\beta_2\dot{f}_2(\dot{f}_1 + \Delta f)L]}{\alpha^2 + [4\pi^2\beta_2\dot{f}_2(\dot{f}_1 + \Delta f)]^2}$$

$$\cdot g(\dot{f}_1 + f)\, g(\dot{f}_2 + f)\, g(\dot{f}_1 + \dot{f}_2 + f)\, g(f)\, d\dot{f}_1\, d\dot{f}_2\, df \tag{6}$$

where L, α, β_2 and γ are the transmission fiber span length (km), power attenuation coefficient[1] (km^{-1}), chromatic dispersion coefficient (ps$^2\cdot$ km^{-1}) and nonlinear coefficient (W$^{-1}\cdot$ km^{-1}) respectively. Similarly for SPM, n_{SPM} is given by

$$n_{\text{SPM}} = p_0^3\, X_{0,0} = p_0^3\, N_s \frac{16}{27}\gamma^2\, R$$

$$\int_{-\infty}^{\infty}\int_{-\infty}^{\infty}\int_{-\infty}^{\infty} \frac{1 + e^{-2L\alpha} - 2e^{-L\alpha}\cos[4\pi^2\beta_2\dot{f}_2\dot{f}_1 L]}{\alpha^2 + [4\pi^2\beta_2\dot{f}_2\dot{f}_1]^2}$$

$$g(\dot{f}_1 + f)\, g(\dot{f}_2 + f)\, g(\dot{f}_1 + \dot{f}_2 + f)\, g(f)\, d\dot{f}_1\, d\dot{f}_2\, df. \tag{7}$$

The values of the nonlinear interference efficiency factor, $X_{i,j}$, were calculated by numerical integration of equations (6) or (7). While the limits of integration are shown as $\pm\infty$ most of the integrand is zero such that for practical numerical integration of equations (6) or (7) df can be limited to $\pm\frac{1}{2}(1 + \text{RRC})\,R$ and that of $d\dot{f}_1$ and $d\dot{f}_2$ can be limited to $\pm(1 + \text{RRC})\,R$, where RRC is the root raised cosine roll off factor defining the signal spectral shape.

The transmission fiber values were set as $\alpha = 0.0507$ km^{-1} ($= 0.22$ dB $\cdot$ km^{-1}), $\beta_2 = -21.3$ ps$^2\cdot$ km^{-1} ($= 16.7$ ps $\cdot$ nm$^{-1}\cdot$ km^{-1}) and $\gamma = 1.3$ W$^{-1}\cdot$ km^{-1}. The signal was assumed to

[1]It should be noted that in this paper α represents the more usual power attenuation coefficient and is thus double the electric field attenuation coefficient used in [15].
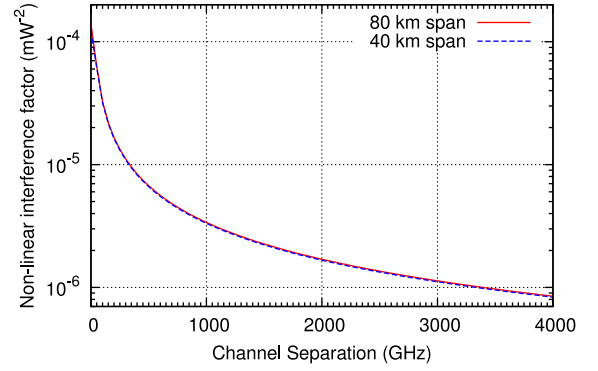

Fig. 1. The nonlinear interference noise efficiency factor, X, for XPM as a function of channel spacing Δf for two span lengths. Note $\Delta f = 0$ refers to SPM.

be a polarization multiplexed signal with $R = 28$ GBaud, that includes a 12% overhead for FEC and framing such that a pre-FEC BER of 4×10^{-3} can be corrected to be error free. The spectral shape was defined by a root raised cosine filter with a roll off factor of $1/2$. Fig. 1 shows the variation of the nonlinear interference efficiency factor as a function of the channel separation for two span lengths. It can be seen that the nonlinear interference efficiency factor, X, shows only slight dependence on span length, L, and decreases proportionally to $\frac{1}{\Delta f}$ for higher channel spacing. Thus the neighboring channels are more significant when it comes to generating nonlinear interference and will give the greatest opportunity for mitigation.

III. Link Optimization

The nonlinear transmission model above was first used to optimize the performance of a single point-to-point optical transmission link. Consider a conventional transmission link where all of the transmitters launch the same signal power, p. Then for a transmission link operating in the nonlinear propagation regime there is an optimum launch power which maximizes the minimum symbol SNR of the worst channel given by [15]

$$p = \sqrt[3]{\frac{n_{\text{ASE}}}{2X_m}} \tag{8}$$

where X_m is given by

$$X_m = \max_i \sum_j X_{i,j} \tag{9}$$

and is the accumulated maximum nonlinear interference on the worst channel. This leads to a maximized minimum symbol SNR is given by

$$\text{SNR}_m = \frac{p}{n_{\text{ASE}} + p^3 X_m}. \tag{10}$$

Consider a link consisting of 8 spans of length 80 km with the transmission fiber parameters as shown in Section II. The transmitter and receiver nodes were estimated to each have 7.25 dB of loss due to the DWDM multiplexers and patching connections compensated by an internal EDFA. All the EDFAs were assumed to have a noise figure of 5 dB (equivalent to an ASE noise contribution on each channel of 5.3×10^{-3} mW at
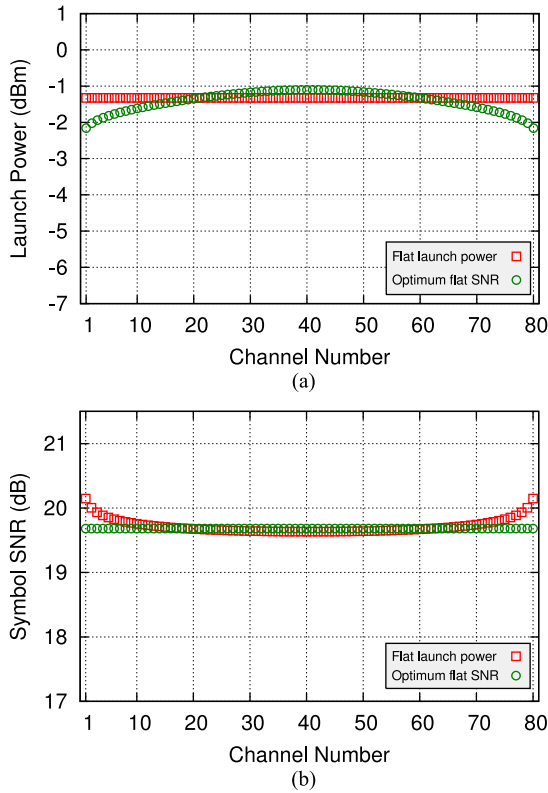
Fig. 2. The launch power a) and symbol SNR b) for each channel under two SNR optimization strategies for the point-to-point link.

Fig. 3. The launch power a) and symbol SNR b) for each channel under two capacity optimization strategies for the point-to-point link.

the receiver). The link was assumed to support 80 channels on a 50 GHz fixed grid at a symbol rate of 28 GBaud and with root raised cosine filtering as described in Section II.

Two launch power strategies where considered: (i) where the launch power was equal for all channels and (ii) when the individual launch powers were optimized to maximize the flat symbol SNR of all the channels. The results are shown in Fig. 2 where the symbol SNR has been calculated using equation (1) for equal launch power and for optimized launch power. The individual channels powers have been optimized iteratively using a Newton–Raphson method while the required SNR is increased to a maximum beyond which no solution to the power optimization is available. For a flat launch power the maximum accumulated nonlinear interference efficiency factor on the center channel, X_m, was found to be 6.7×10^{-3} mW^{-2} such that the optimized flat launch power, p, was 0.74 mW (-1.3 dBm) leading to a minimum symbol SNR just above 19.6 dB. The channels towards the edge of the band show higher SNR since the nonlinear interference is reduced as there are fewer neighboring channels. The individual channel powers have been optimized to maximize the flat symbol SNR of all the channels to just below 19.7 dB. By redistributing the channel powers the minimum symbol SNR has been slightly increased, but by less than 0.1 dB.

Fig. 3 shows the launch power and symbol SNR for each channel under two capacity optimization strategies. In the first strategy we calculated the overall network capacity by maxi-
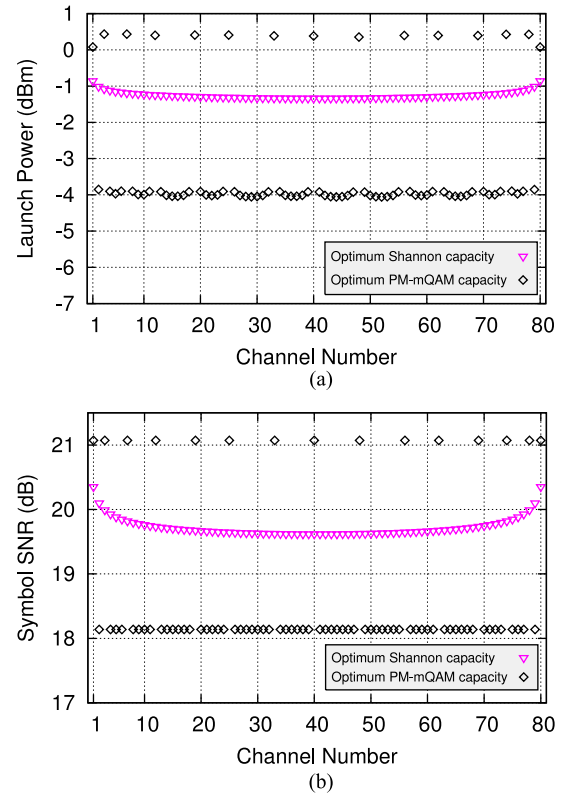
TABLE I
REQUIRED SYMBOL SNR TO ACHIEVE A PRE-FEC BER OF 4×10^{-3} AND ERROR FREE DATA RATE AT 28 GBAUD, INCLUDES 12% OVERHEAD, FOR VARIOUS PM-mQAM MODULATION FORMATS

Format Acronym	Bit Loading (b·Sym^{-1})	Data Rate (Gb·s^{-1})	Required Symbol SNR (dB)
PM-BPSK	2	50	5.5
PM-QPSK	4	100	8.5
PM-8QAM	6	150	12.5
PM-16QAM	8	200	15.1
PM-32QAM	10	250	18.1
PM-64QAM	12	300	21.1

mizing the metric b given by the Shannon capacity equation [29]

$$b = \sum_i \log_2 [\text{SNR}_i + 1] \qquad (11)$$

such that the Shannon capacity of the link is $2b\,R$ where R is the symbol rate and the factor 2 accounts for the polarization multiplexing. The Shannon capacity for this link configuration was found to be 29.4 Tb·s^{-1}, with a maximized minimum SNR of 19.6 dB. According to Table I, which shows the required symbol SNR calculated for an ideal constellation with AWGN to achieve a pre-FEC BER of 4×10^{-3} [30], [31], PM-32QAM modulation could be employed to achieve an overall link capacity of 20 Tb · s^{-1}.

TABLE II
SUMMARY OF THE FOUR POINT-TO-POINT LINK OPTIMIZATION STRATEGIES

Optimization Strategy	Minimum Symbol SNR (dB)	Shannon Capacity (Tb·s^{-1})	PM-mQAM Capacity (Tb·s^{-1})
Flat launch power	19.6	29.4	20.0
Flat SNR	19.7	29.4	20.0
Shannon capacity	19.6	29.4	20.0
PM-mQAM capacity	18.1	27.9	20.8

In the second capacity optimization strategy shown in Fig. 3 we maximized the capacity of the link by using the most spectrally efficient PM-mQAM modulation format that the channel symbol SNR would allow for a given channel launch power distribution. The power of each channel was then optimized to achieve a symbol SNR, and the modulation format chosen from those listed in Table I such that the symbol SNR exceeded the required symbol SNR. For the link under consideration the maximized flat symbol SNR lies between that required for PM-32QAM and PM-64QAM so the optimal link capacity can be achieved for a mixture of these formats. The majority of the channels can support the PM-32QAM modulation format with a minority of channels having sufficient symbol SNR to support the PM-64QAM modulation format. These minority channels were polynomially distributed to try and emulate on average the launch power of the optimized Shannon capacity. The number of higher order format channels was maximized, whilst ensuring the launch power and channel allocations could be optimized to achieve the required symbol SNRs. The maximized PM-mQAM capacity of the link was 20.8 Tb · s^{-1}, which corresponds to a maximized minimum SNR for the PM-32QAM and the PM-64QAM channels of 18.1 and 21.1 dB, respectively.

Table II summaries the optimization strategies along with the minimum symbol SNR, the resultant Shannon capacity and the PM-mQAM capacity based on the modulation formats and required symbol SNR described in Table I. Thus by re-distribution of the launch power between channels the minimum symbol SNR can be improved. By optimizing the launch power to achieve a symbol SNR tailored to a modulation format the capacity of the link can be increased. In the next section these ideas are developed for a three node network where there are significant differences in the transmission distances and SNR values for different connections.

IV. NETWORK OPTIMIZATION I: A THREE-NODE NETWORK

Next we extend the link model to a simple three-node network as illustrated in Fig. 4. The transmission parameters remain as in Section III, however, in addition to the launch and receive nodes the central add-drop node was assumed to have a loss of 14 dB for all signals added, dropped or passed through. This loss is based on a broadcast and select ROADM design with node degree 4 and includes the loss of a 1:4 splitter and a wavelength selective switch. Initially the DWDM channel allocations were grouped with the first half group of 40 channels traversing the whole network and the second half group of 40 channels be-
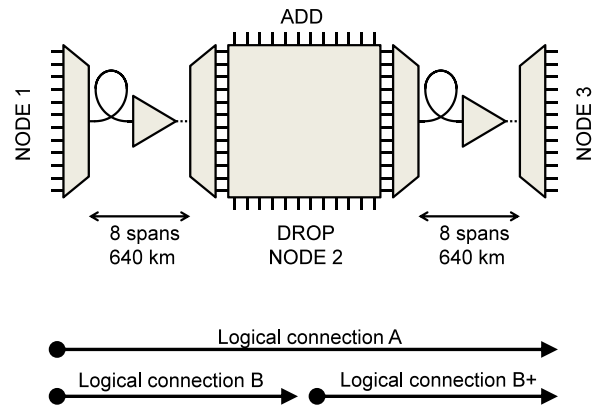

Fig. 4. Outline of the three-node DWDM network, showing the physical and logical connections.
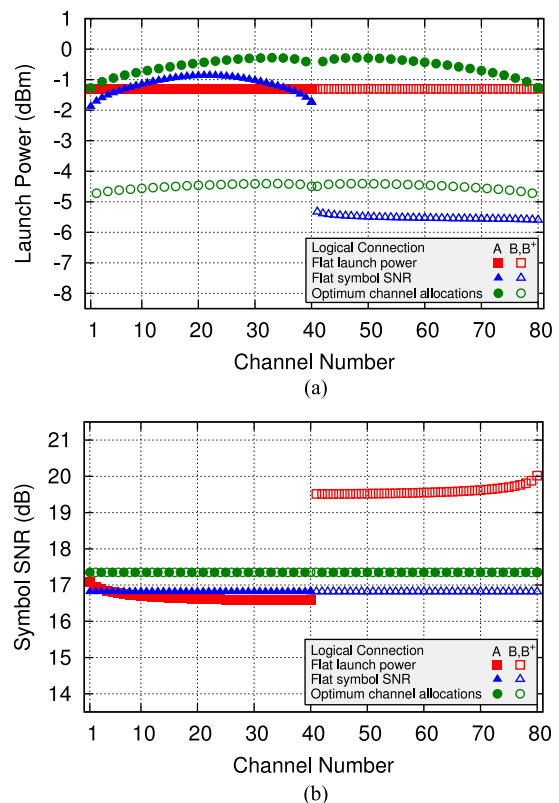

Fig. 5. The launch power a) and symbol SNR b) for each channel under three symbol SNR optimisation strategies for the three node network.

ing dropped with 40 channels added at the central node. The accumulated ASE noise for the signals traversing the longest path from node 1 to node 3 is 10.8×10^{-3} mW. The maximum accumulated nonlinear interference efficiency factor on the center channel, X_m, is a factor of 2 higher than that of the half-length link of Section III and is 13.3×10^{-3} mW^{-2} such that the optimized flat launch power, p, was 0.74 mW (-1.3 dBm), leading to a minimum symbol SNR of 16.6 dB. Fig. 5 shows the optimized launch power and symbol SNR versus channel number for three SNR optimizations. The flat launch power
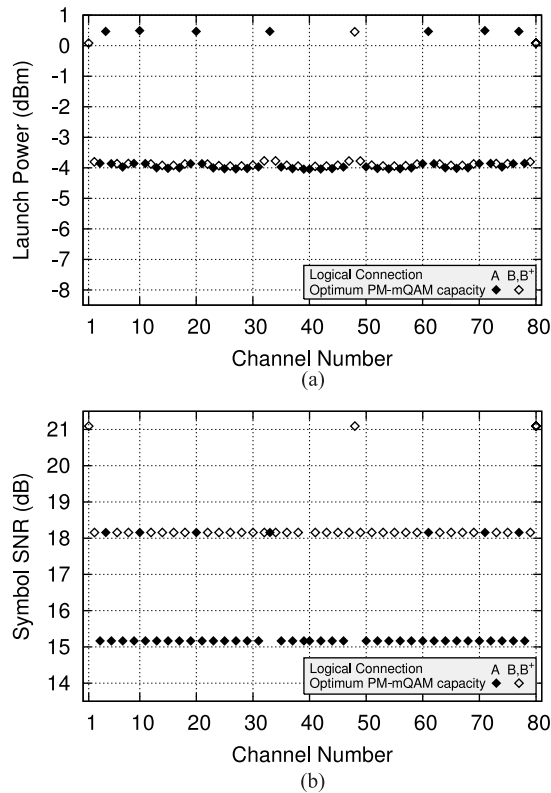
Fig. 6. The launch power a) and symbol SNR b) for a capacity optimisation strategy for the three node network.

Optimization Strategy	Minimum Symbol SNR (dB)	Shannon Capacity (Tb·s^{-1})	PM-mQAM Capacity (Tb·s^{-1})
Flat launch power	16.6, 19.5	12.5, 14.6	8.0, 10.0
Flat SNR, grouped channels	16.8, 16.7	12.6, 12.6	8.0, 8.0
Flat SNR, optimized channel allocations	17.3, 17.3	13.0, 13.0	8.0, 8.0
PM-mQAM capacity	15.2, 18.2	12.9, 12.4	9.2, 9.2

The total network throughput is restricted by the minimum of the A, B or B$^+$ connection capacity under the constraint of uniform capacity between all nodes.

in Section III. The higher power channels have been utilized to balance the capacity of logical connections A and B.

Table III summarises the optimization strategies along with the minimum symbol SNR, the Shannon capacity and the PM-mQAM capacity based on the modulation formats and required symbol SNR described in Section III. It should be noted that logical connections B and B+ have the same channel allocation as these are reused and have the same launch power, SNR and capacity since the network is symmetric with node 2 half way between nodes 1 and 3. Thus re-distributing launch power from the shorter to longer lengths in combination with a correct wavelength allocation can increase the minimum symbol SNR. Also by optimizing the modulation format for a specific connection, depending on its symbol SNR, the bandwidth required for shorter connections has been reduced allowing more bandwidth for longer connections and increasing the overall network throughput. In the next section the advantage of route adaptive modulation format is explored in a larger mesh network.

V. NETWORK OPTIMIZATION II: A MESH NETWORK

To understand the possible capacity gains, through optimization of the transmitter power and modulation format, the 14 node NSF mesh network was investigated [32]. In this initial work the transmitter power is globally optimized assuming flat equal launch power for all the transmitters and fully loaded links. The more complex individual power optimization and channel spectral assignment has been left to future study, preliminary results of which have been presented in [33]. Fig. 7 shows the network topology and link lengths used. The link lengths, Z (km), were calculated from the great circle distance between the nodes, Z_{GC} (km), using [34]

$$Z \begin{cases} = 1.50\,Z_{GC}, & Z_{GC} \leq 1000\,\text{km} \\ = 1500, & 1000\,\text{km} \leq Z_{GC} \leq 1200\,\text{km} \\ = 1.25\,Z_{GC}, & Z_{GC} \geq 1200\,\text{km} \end{cases} \quad (12)$$

where the great circle distance between the nodes was calculated from the latitude and longitude of the nodes using the Haversine

optimization clearly shows that the symbol SNR for the signals traversing the shorter distance are nearly 3 dB higher. By optimizing the individual channel launch power to maximize the minimum flat SNR while keeping the grouped channel allocations leads to a minimum symbol SNR of 16.8 dB. Finally the individual channel launch powers were optimized to maximize the minimum flat SNR with the channel allocations interleaved between the longer and shorter connection giving a minimum symbol SNR of 17.3 dB. This channel allocation pattern has been shown to be the optimum for 12 channels through an exhaustive search of all possible allocations [16], and has been extended here, by inspection, to 80 channels. The full optimization of channel allocations and launch power has increased the minimum channel symbol SNR by 0.7 to 17.3 dB. This improvement in symbol SNR is lower than the 1.3 dB previously achieved [16] due to the inclusion of SPM in the nonlinear interference.

Fig. 6 shows the capacity optimization based on PM-mQAM transmission formats as described in Section III. The maximum uniform capacity where equal traffic is routed between each node pair, was found with 44 channels used for logical connection A and 36 channels used for logical connection B and B+. The majority of channels have a similar launch power, with the logical connections B and B+ able to transmit at a higher modulation rate. It was found a maximum of ten higher power channels could also be accommodated and these were spaced as
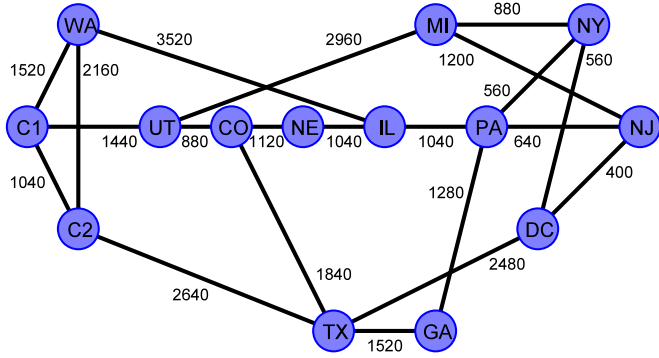
Fig. 7.   14 node NSF mesh network showing fiber link lengths used.

formula [35]

$$Z_{\mathrm{GC}} = 2R_e$$

$$\arcsin\left(\sqrt{\sin^2\left(\frac{\phi_1 - \phi_2}{2}\right) + \cos\left(\phi_1\right)\cos\left(\phi_2\right)\sin^2\left(\frac{\lambda_1 - \lambda_2}{2}\right)}\right) \tag{13}$$

where R_e is the radius of the earth taken as 6367 km and ϕ and λ are the latitude and longitude of the nodes.

The link lengths were rounded to the nearest 80 km, the span length used in this work. Each link within the network consists of a fiber pair, with each fiber able to support 80 DWDM channels on a 50 GHz grid with 28 GBaud symbol rate as in Section III. The amplifier spacing, link and ROADM losses are as in Section III.

The overall aim is to maximize the throughput of the network and analyse its variation for a fixed modulation format compared to a modulation format adapted to the signal quality. In maximising the network throughput, a routing and wavelength assignment problem must also be solved, based on a given traffic demand profile. A normalized traffic demand matrix based on the maximum entropy model [36], [37] was defined as, **T** given by

$$T_{s,d}\begin{cases} \propto e^{\frac{-Z_{s,d}}{Z_0}}, & s \neq d \\ = 0, & s = d \end{cases} \tag{14}$$

where Z_0 is a characteristic traffic distance and $Z_{s,d}$ is the shortest distance between the source, s, and destination, d. This gives a traffic form that is essentially uniform with an exponential distance dependence. It is used here since we have seen in IV. that the symbol SNR has a distance dependence and this traffic model allows the investigation of throughput gains as a function of a characteristic traffic distance. The matrix **T** is normalized such that $\sum_s \sum_d T_{s,d} = 1$ and a demand matrix, **D**, is given by

$$\mathbf{D} = c\,\mathbf{T} \tag{15}$$

where c is a factor defining the total network throughput.

The information capacity of each link can be optimized as in Section III however it is not possible to optimize the information capacity of a route as without the final routing solution we are unaware as to how many channels will interact in each link. So, similar to the LOGON strategy [38], an equal launch power

was used as when all channels launch equal power their exact wavelength allocation will not affect the symbol SNR estimate. The minimum symbol SNR on each route can be obtained from equation (10) which assumes that all the DWDM channels are fully occupied and all signals have the same launch power. The ASE power, n_{ASE}, and nonlinear interference efficiency factors, X_m, in equation (10) are route dependent but easily calculated knowing the transmission losses, using equation (2) and the maximum nonlinear interference efficiency factor $X_m = 0.83 \times 10^{-3}$ mW^{-2}· span^{-1} for the transmission parameters given in Section II.

For the network under consideration the aim is to find the maximum throughput, c, by optimizing the channel allocation and routing. We first find the kth shortest routes between each node pair, where $k = 25$ to limit the overall complexity. For each route the worst case symbol SNR was calculated using equation (10) and the highest order modulation format from those available chosen where the minimum symbol SNR calculated exceeds the modulation formats required symbol SNR. For the fixed modulation case the modulation format was chosen to be PM-QPSK unless no transmission is possible in this format, due to a poor SNR. For the adaptive modulation case the modulation format was chosen from PM-BPSK, PM-QPSK, PM-8QAM, PM-16QAM, PM-32QAM, PM-64QAM using the values from Table I. Given the modulation format the capacity of each channel over the route can be calculated.

The channel routing allocation problem was solved using IBM CPLEX as a mixed-integer linear programming, MILP, problem. There are two common ILP formulations: based on flow and on routes [39], [40]. Since in the adaptive modulation case the channel capacity is route-dependent we use the latter here. The demand matrix was assumed to be symmetric, $D_{s,d} = D_{d,s}$, and in fiber pairs, so that the problem can be solved for $d > s$ only. The MILP problem can be described as follows.

Parameters
- s,d: the source and destination nodes $\in 1, 14$,
- l: a link $\in 1, 21$,
- w: a DWDM channel $\in 1, 80$,
- $T_{s,d}$: the normalized traffic flow between source, s, and destination,d,
- $r_{s,d,k}$: the kth shortest route between source, s, and destination,d,
- $\delta^L_{s,d,k,l}$: is set to 1 if route $r_{s,d,k}$ traverses link l, 0 otherwise,
- $\mathrm{SNR}_{s,d,k}$: the symbol SNR for transmission over route $r_{s,d,k}$,
- $C_{s,d,k}$: the capacity of transmission over route $r_{s,d,k}$, it is taken as the capacity of the highest order modulation format from the set of used modulation formats where the route SNR, $\mathrm{SNR}_{s,d,k}$ exceeds the modulation formats' required SNR. Routes $r_{s,d,k}$ where $C_{s,d,k} = 0$ were removed from the problem before optimization to reduce the complexity.

Variables
- c: the total throughput of the network as defined by (15),
- $F_{s,d,k}$: the number of transceivers using route $r_{s,d,k}$,
- $\delta^F_{s,d,k,w}$: is 1 if a transceiver for route $r_{s,d,k}$ uses DWDM channel w, 0 otherwise.
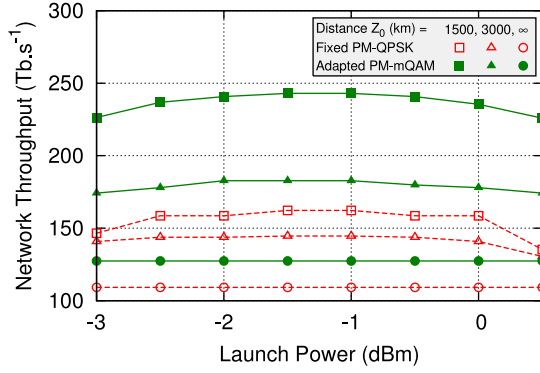
Fig. 8.   The maximum network throughput for three characteristic traffic distances and for fixed PM-QPSK or route optimized PM-mQAM as a function of launch power, with the wavelength continuity constraint relaxed.

First, the relaxed optimization problem was considered, where the wavelength continuity constraint is disregarded. This is equivalent to the physical situation where an unlimited number of wavelength converters is available at each node. Optimize c as a continuous variable and $F_{s,d,k}$ as integer variables to maximize c as $c_{\mathrm{relax,max}}$ subject to the total capacity between the source and destination nodes exceeding the demand

$$cT_{s,d} - \sum_k F_{s,d,k}C_{s,d,k} <= 0 \qquad \forall \quad s, d > s \qquad (16)$$

and that the number of channels does not exceed 80 in any link l

$$\sum_k \sum_s \sum_{d>s} F_{s,d,k}\delta^L_{s,d,k,l} <= 80 \qquad \forall \quad l. \qquad (17)$$

Then we introduce the wavelength continuity constraint [40] and re-solve. Optimize c as a continuous variable and $\delta^F_{s,d,k,w}$ as a binary variable to maximize c as c_{max} subject to the total capacity between the source and destination nodes exceeding the demand

$$cT_{s,d} - \sum_w \sum_k \delta^F_{s,d,k,w}C_{s,d,k} <= 0 \qquad \forall \quad s, d > s \quad (18)$$

and that the number of signals occupying DWDM channel, w, in any link, l, does not exceed 1,

$$\sum_k \sum_s \sum_{d>s} \delta^F_{s,d,k,w}\delta^L_{s,d,k,l} <= 1 \qquad \forall \quad l, w. \qquad (19)$$

The constraint that $c \le c_{\mathrm{relax,max}}$ is included to reduce the solution space for the MILP solver.

Initially the relaxed problem alone was solved to assess the ideal launch power since this could be solved in minutes. The maximum network throughput $c_{\mathrm{relax,max}}$ was found for different launch powers, for the characteristic traffic distances, $Z_0 = 1500, 3000$ or, ∞, each for either fixed PM-QPSK modulation or route optimized modulation from Table I. Fig. 8 shows the results and indicates that a launch power of ≈ -1.5 dBm is optimal for this network as it maximizes the throughput for all cases.

Solutions to the DWDM channel wavelength and routing problem were initially made with the fixed modulation format

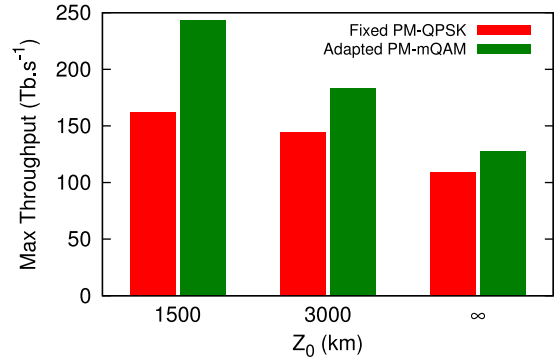| Characteristic Distance	Maximum Network throughput (Tb·s^{-1})	
	Fixed PM-QPSK	Adapted PM-mQAM
$Z_0 = 1500$ km	162.2	242.9
$Z_0 = 3000$ km	144.6	182.8
$Z_0 = \infty$ km	109.2	127.4

Fig. 9.   The maximum network throughput for three characteristic traffic distances and for two network configurations: fixed PM-QPSK modulation on all routes and route SNR adapted PM-mQAM.

chosen as PM-QPSK, as this is suitable for all source destination pairs. The modulation format for each route was then adapted by choosing from the larger set of PM-BPSK, PM-QPSK, PM-8QAM, PM-16QAM PM-32QAM and PM-64QAM as detailed in Table I and the DWDM channel and routing problem resolved to find a new maximum throughput, c_{max}.

Table IV and Fig. 9 show the maximum network throughput for a fixed modulation format and a route SNR adapted modulation format for three characteristic traffic distances, Z_0, as defined in equation (14). It shows that by moving to an adaptive transmission format the network can support between 17 and 50% more traffic depending on the traffic characteristic distance, Z_0. The gains are larger for shorter characteristic distances as these can make better use of higher order modulation formats on shorter routes, where the symbol SNR is higher.

The network throughput gains are not as large as those predicted by Korotky *et al.* [37] who reported throughput gains of between 70% and 150% for a similar diameter mesh network. It should be noted that they define the network throughput gain as the increase in traffic when moving from fixed to adapted modulation format for a fixed number of *a priori* routed connections and not as in our case for a fixed traffic profile. Maintaining the number of connections while adapting their modulation format will lead to larger gains in network throughput as the shorter connections will dominate the gains changing the traffic profile. For traffic demand with a characteristic distance $Z_0 = 1524$ km, they report a throughput gain of 70% for an SNR-adapted modulation format, similar within the difference noted above, to the value of 50% obtained in this work.

Recently, corrections to the GN model [23] or alternative models have been proposed [22], which result in a modulation format dependence of the nonlinear interference noise. The GN model used in this work leads to an overestimation of nonlinear interference noise particularly for PM-QPSK operating over short distances [22], [23]. In an optical network using adaptive modulation, the impact is reduced, since PM-QPSK would only be used for longer distances where the corrections to the GN model are less significant. To quantify the effect of these corrections on the network throughput, we re-ran the MILP using the proposed corrections in [22], [23] and found that the improvement in network throughput was less than 1% for the network considered. We attribute this weak dependence of the network throughput between the original and corrected GN model as being due to the integer limitation on the cardinality of the modulation format, and the use of adaptive modulation, resulting in signals with higher modulation order, that reduce the significance of the corrections, operating over shorter distances. In this case the maximum overestimation error, for the shortest link of 5 spans which utilises PM-64 QAM, is less than 0.5 dB (in contrast PM-QPSK would be used for 40 spans or more with the correction being negligible). Naturally for smaller networks, or those utilising adaptive modulation and coding in order to smooth the transitions between SNR requirements of the different modulations, the impact of the corrections in the GN model may warrant further consideration. This will be considered as part of our future work.

VI. CONCLUSION

This paper has described a simplified Gaussian noise model approach for the rapid calculation of signal quality. The approach is intended for polarization multiplexed coherent optical transmission in dispersion uncompensated networks and allows the calculation of signal quality depending on the individual signal power and WDM channel assignments, with the aim of maximizing the overall network capacity.

It was shown that through correct wavelength channel assignment, gains in the SNR margins can be achieved. The gains can be used to increase network data throughput by adapting the modulation format to the quality of transmission. These results highlight that the launch power should be optimized to maximize the utilization of network resources. WDM channel assignment decisions are influenced by the physical channel characteristics and the presence of nonlinearities, as well as the more usual routing continuity constraints.

The proposed approach and the achievable data throughput was investigated and applied to the 14-node NSF mesh network. The transmission model was used to find the worst case SNR of each route and this was used to set the transmission format for each route. The routing and wavelength allocation problem was solved using MILP to maximize the network throughput. It was shown that by adapting the transmission formats for the different routes through the network the maximum throughput can be increased by between 17% and 50%, depending on the characteristic traffic distance. The larger gains in data throughput can be achieved when the characteristic traffic distance is

small, allowing greater use of higher-order modulation formats. Indeed the assumptions on the traffic demand significantly impacts the achievable capacity gains and needs further examination.

In order to maximize the use of all the available installed optical fiber infrastructure the transmitter parameters should be optimized as part of the routing and spectral assignment algorithm. Optimization of the launch power and modulation format has been demonstrated here to achieve gains in data throughput for the NSF mesh network. The optimization of individual transmitter launch power and modulation format with routing and spectral assignment was shown to improve data throughput for simple networks and has recently been extended to show further improvements in data throughput for the NSF mesh network [33].

REFERENCES

[1] (2009, Aug.). Minnesota Internet Traffic Studies (MINTS). University of Minnesota. [Online]. Available: http://www.dtc.umn.edu/mints/home.php

[2] (2011, Jun.). Cisco Visual Networking Index. Cisco. [Online]. Available: http://www.cisco.com/go/vni

[3] (2013, Nov.). Monthly Performance Pack. BBC iPlayer. [Online]. Available: http://downloads.bbc.co.uk/mediacentre/iplayer/iplayer-performance-nov13.pdf

[4] S. Baroni and P. Bayvel, "Wavelength requirements in arbitrarily connected wavelength-routed optical networks," *J. Lightw. Technol.*, vol. 15, no. 2, pp. 242–251, Feb. 1997.

[5] M. Jinno, H. Takara, B. Kozicki, Y. Tsukishima, Y. Sone, and S. Matsuoka, "Spectrum-efficient and scalable elastic optical path network: Architecture, benefits, and enabling technologies," *IEEE Commun. Mag.*, vol. 47, no. 11, pp. 66–73, Nov. 2009.

[6] O. Gerstel, M. Jinno, A. Lord, and S. J. B. Yoo, "Elastic optical networking: A new dawn for the optical layer?" *IEEE Commun. Mag.*, vol. 50, no. 2, pp. s12–s20, Feb. 2012.

[7] B. Kozicki, H. Takara, Y. Sone, A. Watanabe, and M. Jinno, "Distance-Adaptive spectrum allocation in elastic optical path network (SLICE) with bit per symbol adjustment," presented at the Opt. Fiber Commun. Conf., San Diego, CA, USA, 2010, Paper OMU3.

[8] M. Jinno, B. Kozicki, H. Takara, A. Watanabe, Y. Sone, T. Tanaka, and A. Hirano, "Distance-adaptive spectrum resource allocation in spectrum-sliced elastic optical path network," *IEEE Commun. Mag.*, vol. 48, no. 8, pp. 138–145, Aug. 2010.

[9] R. Schmogrow, D. Hillerkuss, M. Dreschmann, M. Huebner, M. Winter, J. Meyer, B. Nebendahl, C. Koos, J. Becker, W. Freude, and J. Leuthold, "Real-Time software-defined multiformat transmitter generating 64QAM at 28 GBd," *IEEE Photon. Technol. Lett.*, vol. 22, no. 21, pp. 1601–1603, Nov. 2010.

[10] H. Y. Choi, T. Tsuritani, and I. Morita, "BER-adaptive flexible-format transmitter for elastic optical networks," *Opt. Exp.*, vol. 20, no. 17, pp. 18 652–18 658, Aug. 2012.

[11] K. Roberts and C. Laperle, "Flexible Transceivers," presented at the 38th Eur. Conf. Expo. Opt. Commun., Amsterdam, The Netherlands, 2012, Paper We.3.A.3.

[12] H. Cukurtepe, M. Tornatore, A. Yayimli, and B. Mukherjee, "Impairment-aware lightpath provisioning in mixed line rate networks," in *Proc. IEEE Int. Conf. Adv. Netw. Telecommun. Syst.*, Dec. 2012, pp. 18–23.

[13] A. Nag, M. Tornatore, and B. Mukherjee, "Optical network design with mixed line rates and multiple modulation formats," *J. Lightw. Technol.*, vol. 28, no. 4, pp. 466–475, Feb. 2010.

[14] A. Nag, M. Tornatore, and B. Mukherjee, "Power management in mixed line rate optical networks," presented at the Integr. Photon. Res. Silicon Nanophoton. Switching , Monterey, CA, USA, Paper PTuB4.

[15] P. Poggiolini, "The GN model of non-linear propagation in uncompensated coherent optical systems," *J. Lightw. Technol.*, vol. 30, no. 24, pp. 3857–3879, Dec. 2012.

[16] D. J. Ives and S. J. Savory, "Transmitter optimized optical networks," presented at the Opt. Fiber Commun. Conf./Nat. Fiber Opt. Eng. Conf., Anaheim, CA, USA, 2013, Paper JW2A.64.

[17] A. Splett, C. Kurtske, and K. Petermann, "Ultimate transmission capacity of amplified optical fiber communication systems taking into account fiber nonlinearities," presented at the Eur. Conf. Opt. Commun., Montreux, Switzerland, 1993, Paper MoC2.4.

[18] P. P. Mitra and J. B. Stark, "Nonlinear limits to the information capacity of optical fibre communications." *Nature*, vol. 411, no. 6841, pp. 1027–1030, Jun. 2001.

[19] A. Carena, G. Bosco, V. Curri, P. Poggiolini, M. T. Taiba, and F. Forghieri, "Statistical characterization of PM-QPSK signals after propagation in uncompensated fiber links," presented at the Eur. Conf. Exhib. Opt. Commun., Amsterdam, The Netherlands, Sep. 2010, Paper P4.07.

[20] F. Vacondio, O. Rival, C. Simonneau, E. Grellier, A. Bononi, L. Lorcy, J.-C. Antona, and S. Bigo, "On nonlinear distortions of highly dispersive optical coherent systems," *Opt. Exp.*, vol. 20, no. 2, pp. 1022–1032, Jan. 2012.

[21] R. Dar, M. Feder, A. Mecozzi, and M. Shtaif, "Properties of nonlinear noise in long, dispersion-uncompensated fiber links," *Opt. Exp.*, vol. 21, no. 22, pp. 25685–25699, Nov. 2013.

[22] R. Dar, M. Feder, A. Mecozzi, and M. Shtaif, "Accumulation of nonlinear interference noise in fiber-optic systems," *Opt. Exp.*, vol. 22, no. 12, pp. 14 199–14 211, Jun. 2014.

[23] A. Carena, G. Bosco, V. Curri, Y. Jiang, P. Poggiolini, and F. Forghieri, "EGN model of non-linear fiber propagation," *Opt. Exp.*, vol. 22, no. 13, pp. 16335–16362, Jun. 2014.

[24] D. A. A. Mello, A. N. Barreto, T. C. de Lima, T. F. Portela, L. Beygi, and J. M. Kahn, "Optical networking with variable-code-rate transceivers," *J. Lightw. Technol.*, vol. 32, no. 2, pp. 257–266, Jan. 2014.

[25] H. Kogelnik and A. Yariv, "Considerations of noise and schemes for its reduction in laser amplifiers," *Proc. IEEE*, vol. 52, no. 2, pp. 165–172, Feb. 1964.

[26] A. Yariv, "Signal-to-noise considerations in fiber links with periodic or distributed optical amplification," *Opt. Lett.*, vol. 15, no. 19, pp. 1064–1066, Oct.1990.

[27] P. Poggiolini, G. Bosco, A. Carena, V. Curri, Y. Jiang, and F. Forghieri, "The GN-model of fiber non-linear propagation and its applications," *J. Lightw. Technol.*, vol. 32, no. 4, pp. 694–721, Feb. 2014.

[28] A. Carena and G. Bosco, "Impact of the transmitted signal initial dispersion transient on the accuracy of the GN-model of non-linear propagation," presented at the Eur. Conf. Expo. Opt. Commun., London, U.K., 2013, Paper Th.1.D.4.

[29] C. E. Shannon, "Communication in the presence of noise," *Proc. Inst. Radio Eng.*, vol. 37, no. 1, pp. 10–21, Jan. 1949.

[30] K. Cho and D. Yoon, "On the general BER expression of one- and two-dimensional amplitude modulations," *IEEE Trans. Commun.*, vol. 50, no. 7, pp. 1074–1080, Jul. 2002.

[31] P. K. Vitthaladevuni, M.-S. Alouini, and J. Kieffer, "Exact BER computation for cross QAM constellations," *IEEE Trans. Wireless Commun.*, vol. 4, no. 6, pp. 3039–3050, Nov. 2005.

[32] R. Ramaswami and K. Sivarajan, "Design of logical topologies for wavelength-routed all-optical networks," presented at the IEEE Conf. Comput. Commun., Boston, MA, USA, Apr. 1995, Paper 10c.4.1.

[33] D. J. Ives, P. Bayvel, and S. J. Savory, "Physical layer transmitter and routing optimization to maximize the traffic throughput of a nonlinear optical mesh network," in *Proc. Opt. Netw. Design Model.*, Stockholm, Sweden, 2014, pp. 168–173.

[34] *Network Aspects (NA); Availability Performance of Path Elements of International Digital Paths*, ETSI Standard EN 300 416, Aug. 1998.

[35] J. P. Snyder, "*Map Projections—A Working Manual*," U.S. Geological Survey Professional Paper 1395, U.S. Government Printing Office, Washington D.C., USA, 1987.

[36] S. K. Korotky and K. N. Oikonomou, "Scaling of the most likely traffic patterns of hose- and cost-constrained ring and mesh networks," *J. Opt. Netw.*, vol. 7, no. 6, pp. 550–563, Jun. 2008.

[37] S. K. Korotky, R.-J. Essiambre, and R. W. Tkach, "Expectations of optical network traffic gain afforded by bit rate adaptive transmission," *Bell Labs Tech. J.*, vol. 14, no. 4, pp. 285–295, Feb. 2010.

[38] P. Poggiolini, G. Bosco, A. Carena, R. Cigliutti, V. Curri, F. Forghieri, R. Pastorelli, and S. Piciaccia, "The LOGON Strategy for low-complexity control plane implementation in new-generation flexible networks," presented at the Opt. Fiber Commun. Conf., Anaheim, CA, USA, Mar. 2013, Paper OW1H.3.

[39] D. Banerjee and B. Mukherjee, "A practical approach for routing and wavelength assignment in large wavelength-routed optical networks," *IEEE J. Select. Areas Commun.*, vol. 14, no. 5, pp. 903–908, Jun. 1996.

[40] N. Wauters and P. Demeester, "Design of the optical path layer in multi-wavelength cross-connected networks," *IEEE J. Select. Areas Commun.*, vol. 14, no. 5, pp. 881–892, Jun. 1996.

David J. Ives received the B.Sc. degree in physics from the University of Birmingham, Birmingham, U.K., in 1988, and the MRes degree in photonic systems development from the University College London, London, U.K., in 2011. He is currently working toward the Ph.D. degree with the Optical Networks Group, Department of Electronic and Electrical Engineering, University College London, London.

He spent 21 years at the National Physical Laboratory, Teddington, U.K., as part of the Photonics Group, where he developed techniques for the characterization of optical fiber waveguides and the calibration of optical fiber test equipment. In September 2010, he joined the Center for Doctoral Training in Photonic Systems Development. His research interests include physical layer optical network optimization to improve network resource utilization and maximizing the throughput. He is a Student Member of OSA.

Polina Bayvel received the B.Sc. degree in engineering and Ph.D. degree in electronic and electrical engineering from the University of London, London, U.K., in 1986 and 1990, respectively. In 1990, she was with the Fiber Optics Laboratory, General Physics Institute, Moscow (Russian Academy of Sciences), Russia, under the Royal Society Postdoctoral Exchange Fellowship. She was a Principal Systems Engineer with STC Submarine Systems, Ltd., London and Nortel Networks, Harlow, U.K., and Ottawa, ON, Canada, where she was involved in the design and planning of optical fiber transmission networks. During 1994–2004, she held a Royal Society University Research Fellowship at University College London (UCL), and she became a Chair in Optical Communications and Networks in 2002. She is currently the Head of the Optical Networks Group, UCL. She has authored or coauthored more than 300 refereed journal and conference papers. Her research interests include wavelength-routed optical networks, high-speed optical transmission, and the mitigation of fiber nonlinearities.

She is a Fellow of the Royal Academy of Engineering (FREng.), the Optical Society of America, the U.K. Institute of Physics, and the Institute of Engineering and Technology. She received the Royal Society Wolfson Research Merit Award (2007–2012), IEEE Photonics Society Engineering Achievement Award in 2013 and Royal Society Clifford Patterson Prize Lecture and Medal in 2014.

Seb J. Savory received the M.Eng., M.A., and Ph.D. degrees in engineering from the University of Cambridge, Cambridge, U.K., in 1996, 1999, and 2001, respectively, and the M.Sc. degree in mathematics from the Open University, Milton Keynes, U.K., in 2007. His interest in optical communications began in 1991, when he joined Standard Telecommunications Laboratories, Harlow, U.K., prior to being sponsored through his undergraduate and postgraduate studies, after which he rejoined Nortel's Harlow Laboratories in 2000. In 2005, he joined the Optical Networks Group at University College London, where he held a Leverhulme Trust Early Career Fellowship from 2005 to 2007, before being appointed as a Lecturer in 2007, and subsequently, a Reader in Optical Fibre Communication in 2012. In 2014, he received a Royal Academy of Engineering/Leverhulme Trust Senior Research Fellowship to conduct research in "realising the capacity in fibre-optic networks with uncertainty and nonlinearity".